

Evaluation of antibacterial textile covered by layer-by-layer coating and loaded with chlorhexidine for wound dressing application

Francois Aubert-Viard, Alejandra Mogrovejo Valdivia, Nicolas Tabary, Mickael Maton, Feng Chai, Christel Neut, Bernard Martel, Nicolas Blanchemain

▶ **To cite this version:**

Francois Aubert-Viard, Alejandra Mogrovejo Valdivia, Nicolas Tabary, Mickael Maton, Feng Chai, et al.. Evaluation of antibacterial textile covered by layer-by-layer coating and loaded with chlorhexidine for wound dressing application. Materials Science and Engineering: C, 2019, Materials Science and Engineering: C, 100, pp.554-563. 10.1016/j.msec.2019.03.044 . hal-02114423

HAL Id: hal-02114423
https://hal.univ-lille.fr/hal-02114423

Submitted on 22 Oct 2021

HAL is a multi-disciplinary open access archive for the deposit and dissemination of scientific research documents, whether they are published or not. The documents may come from teaching and research institutions in France or abroad, or from public or private research centers.

L'archive ouverte pluridisciplinaire **HAL**, est destinée au dépôt et à la diffusion de documents scientifiques de niveau recherche, publiés ou non, émanant des établissements d'enseignement et de recherche français ou étrangers, des laboratoires publics ou privés.



Distributed under a Creative Commons Attribution - NonCommercial 4.0 International License

Version of Record: https://www.sciencedirect.com/science/article/pii/S0928493118329515
Manuscript_52136b5af22c788858d1a21c1688ab5e

Evaluation of antibacterial textile covered by Layer-by-Layer coating and loaded with Chlorhexidine for wound dressing application

François Aubert-Viard[a,b], Alejandra Mogrovejo-Valdivia[a], Nicolas Tabary[b], Mickael Maton[a], Feng Chai[a], Christel Neut[c], Bernard Martel[b], Nicolas Blanchemain[a*]

[a] Univ. Lille, INSERM, CHU Lille, U1008 - Controlled Drug Delivery Systems and Biomaterials, F-59000 Lille, France

[b] Univ. Lille, CNRS UMR8207, UMET - Unité Matériaux et Transformations, F-59655 Villeneuve D'Ascq, France

[c] Univ. Lille, INSERM, CHU Lille, U995- LIRIC - Lille Inflammation Research International Center, F-59000 Lille, France

* Corresponding author. Dr. Nicolas Blanchemain

E-mail : nicolas.blanchemain@univ-lille2.fr

Address: INSERM U1008, Controlled Drug Delivery Systems and Biomaterials, College of Pharmacy, University Lille 2, 59006 Lille, France

Tel.: +33 320 62 69 75

Fax: +33 320 62 68 54

© 2019 published by Elsevier. This manuscript is made available under the CC BY NC user license
https://creativecommons.org/licenses/by-nc/4.0/

Abstract

The aim of this work is to design a wound dressing able to release chlorhexidine (CHX) as antiseptic agent, ensuring long-lasting antibacterial efficacy during the healing. The textile nonwoven (polyethylene terephthalate) (PET) of the dressing was first modified by chitosan (CHT) crosslinked with genipin (Gpn). Parameters such as the concentration of reagents (Gpn and CHT) but also the crosslinking time and the working temperature were optimized to reach the maximal positive charges surface density. This support was then treated by the layer-by-layer (LbL) deposition of a multilayer system composed of methyl-beta-cyclodextrin polymer (PCD) (anionic) and CHT (cationic). After a thermal treatment to stabilize the LbL film, the textiles were loaded with CHX as antiseptic agent. The influence of the thermal treatment i) on the cytocompatibility, ii) on the degradation of the multilayer system, iii) on CHX sorption and release profiles and iv) on the antibacterial activity of the loaded textiles was studied.

Keywords

Antibacterial textile, Chitosan, Genipin, cytocompatibility, Cyclodextrin, Chlorhexidine, Layer-by-Layer

1. Introduction

Skin is the largest (1.2 to 2.3 m²) and heaviest (10 to 16% of the total body mass) organ of the human body and is structured in three layers: the epidermis, the dermis and the hypodermis from the most superficial to the deepest. This structure provides to the skin several functions: sensitivity (temperature, touch of solids, liquids), thermal regulation of the body and protective barrier against physical, chemical and foreign microorganisms aggressions [1]. Various factors may damage this protection such as wounds, bedsores or scars that pave the way for pathogens and subsequent complications.

Indeed, infections provoke tissues necrosis, subsequently delay the healing process and extend the healing period with dramatic consequences for the patient. The most frequent harmful germ is *Staphylococcus aureus* (24 to 50%) [2–4]. Nevertheless, in most of cases the infection is poly-microbial with the presence of other bacterial strains such as *Staphyloccocus epidermidis*, *Escherichia coli* or *Pseudomonas aeruginosa* [5–10]. Infected wounds request the use of antibacterial dressings to eradicate bacterial colonization and eliminate biofilm in order to allow the beginning of healing process in a second time. As necrotic tissues are poorly irrigated, local treatments give better results than systemic administration. In the state-of-the art, antibacterial dressings present biocide functionality through contact killing provided by specific chemical groups such as alkyl ammonium groups [11] or through the release of antiseptic agents such as chlorhexidine (CHX), triclosan, silver salts or nanoparticles [12,13].

Chitosan (CHT) is a polymer of choice for use in wound dressings due to its biocompatible [14,15] biodegradable, bacteriostatic, mucoadhesive and hemostatic properties [16–20]. CHT is a natural polysaccharide obtained from deacetylation of chitin extracted from crustacean shells and composed by D-2-deoxy-2-acetyl-glucosamine and D-2-deoxy-glucosamine units linked by β (1→4) binding. The presence of basic amino functions ($-NH_2$) confers to CHT a

polycationic character in acidic conditions due to their transformation in ammonium groups (-NH_3^+). Besides, CHT benefits from the high chemical reactivity of its amino groups toward crosslinking reactions by using di-functional molecules such as glutaraldehyde, polyethylene glycol epoxy polymer [21–23] or various compounds like polycarboxylic acids[24] and in particular genipin (Gpn) used in the present study [15,25]. As a matter of fact, it is well known that most of the crosslinking agents and especially di-aldehydes are toxic, making them unsuitable for biomedical applications. On contrary, Gpn extracted from fruits of *Gardenia jasminoïdes Ellis* is commonly used in pharmaceutical or food industry as pigment precursor for food dyeing. Besides, Gpn readily reacts with primary amino groups of CHT and proteins leading to their crosslinking [26–28]. This compound is recognized to be less cytotoxic than most of crosslinking agents, especially glutaraldehyde [15] and is therefore acceptable for biomaterials application.

Moreover, the crosslinking reaction by Gpn occurs in mild conditions *i.e.* at room temperature, which are favourable to highly heat-sensitive compounds such as proteins or substrates such as textiles. Thus, Liu & Huang have developed a bilayer dressing based on soy protein and CHT film crosslinked by Gpn to improve epithelialization and repair of injuries [28]. More recently, Martin *et al* reported coating of a textile support by a polyelectrolyte multilayer (PEM) system obtained from the self-assembly of CHT and an anionic cyclodextrin polymer (PCD) bearing carboxylate groups [29,30]. The cohesion of such nanostructured system was directed by the formation of polyelectrolyte complexes (PEC) formed between CHT and PCD and its stability in aqueous media depended on the pH and on ionic strenght of the medium [31].

The incorporation or immobilization of antibacterial agents (methylene blue, CHX, metallic ions) on wound dressing is used to prevent wound infections [32]. CHX is a biguanide compound widely used for the local bucco-pharyngal, cutaneous antisepsis with a broad-

spectrum activity and can be used in association with other antibacterial compounds such as benzalkonium chloride in particular in Biseptine® principally used for cutaneous application. The association of CHX with other compounds like iodine has also been reported to improve the antibacterial effect of the CHX (synergic effect) [33].

This study reports the elaboration of an antibacterial textile coated by a first layer of CHT immobilized by crosslinking with Gpn, onto which a polyelectrolyte multilayer (PEM) film was built up, consisting of the self-assembled layers of anionic PCD and cationic CHT. The antibacterial activity of the modified textiles was determined by release-killing effect after loading the PEM system with CHX. In our concept, the PCD is expected not only to provide enhanced reservoir and sustained release properties to the PEM system thanks to the CHX-cyclodextrin (CD) inclusion complexes formation and to its slow dissociation.

This paper reports the impact of sample preparation conditions on the first crosslinked CHT layer with Gpn, which was necessary to provide cationic sites firmly anchored to the neutral polyester fibres, and then the PEM build-up construction will be investigated. The *in vitro* CHX kinetic of release is studied in parallel with the *in vitro* antibacterial tests on *S. aureus*. As this support is destined for contact with superficial and deep tissues composing the skin, an evaluation of the cytocompatibility of functionalized textiles was also conducted.

2. Materials and methods

2.1. Materials and reagents

The textile support used was a non-woven polyethylene terephthalate (PET, NSN 365) provided by PGI-Nordlys (Bailleul, France). The density of PET was 76 g/cm² and the thickness 0.24 mm. Before chemical modification, the textiles were thoroughly washed by three successive cycles of soxhlet extraction with isopropanol and distilled water. PET was chosen for its biocompatibility, low price and wide use in commercially available wound dressings.

Gpn, acetic acid, CHT and Phosphate Buffered Saline (PBS) were purchased from Sigma Aldrich (Saint Louis, USA). CHT was a low molecular weight grade (batch N° SLBG1673V, 190 kDa, viscosity: 20-300, in 1%v/v acetic acid) with a degree of deacylation (DD) of 80% +/-5% (according to supplier) and the calculated NH_2 content was 5.0 +/-0.25 mmol/g. PBS solution was prepared by dissolving one tablet in 200 mL of ultrapure water (Pure Lab Flex Elga, Veolia). The final concentration was 0.01 M phosphate buffer, 0.0027 M potassium chloride and 0.137 M sodium chloride (pH 7.4 at 25 °C). CHX was purchased from INRESA (Bartenheim, France)

2-O-Methyl β-cyclodextrins (MeβCD Crysmeb®, DS = 0.50) was purchased from Roquette (Lestrem, France). Anionic water-soluble PCD was synthetized according to a method patented by Weltrowski et al. [34]. Citric acid as crosslinking agent, sodium hypophosphite as catalyst and MeβCD in respective weight ratio 10/3/10 (g in 100 mL) were dissolved in water. After water removal using a rotative evaporator, the resulting solid mixture was then cured at 140°C during 30 min under vacuum. Water was then added and the resulting suspension was filtered, and dialyzed during 72 h in water using 6–8 kDa membranes (SPECTRAPOR 1, Spectrumlabs). Finally, the water-soluble anionic CD polymer (PCD) was recovered after freeze drying. The weight composition of PCD, was 74 wt.% in MeβCD moieties (determined

by 1H NMR) and the calculated carboxylate groups content was 2.7 +/-0.3 mmol/g. The molecular mass in number (Mn) of PCD was 8 000 g/mol, measured by size exclusion chromatography SEC) in water equipped with a light scattering detector.

2.2. Chitosan fixation on PET with genipin (PET-CHT)

CHT-1% (w/v) and CHT-2.5% (w/v) were obtained by dissolving CHT in 1% (v/v) acetic acid. Gpn was solubilised in distilled water to obtain final concentrations of 0.01; 0.05; 0.1 and 0.5% (w/v) after mixing with CHT solution. The virgin PET textile (5*5cm) was weighed on a precision balance (+/-10^{-4}g, Kern, Balingen, Germany) (initial weight (w_i)), impregnated in the different CHT/Gpn solutions and roll-padded (Roaches, England). Samples were placed in an incubator at 25°C under wet atmosphere (RH-100%) for 48 hours, where crosslinking reaction occurred. The textiles were finally washed in acetic acid (1% (v/v), 20 min) and ultrapure water (20 min, 2 times) under sonication to remove the unreacted CHT and Gpn, dried at 90°C for 1 hour and weighed (w_f). The degree of functionalization was calculated by the weight gain:

Eq. 1: $$\textbf{Weight gain (\%)} = \frac{W_f - W_i}{W_i} \times 100$$

where w_i and w_f represent the weight of the nonwoven PET samples before and after their modification with CHT-Gpn (named PET-CHT), respectively.

2.3. Layer-by-layer coating (PET-CHT-PEMn).

The multilayer assembly was built using the dip-coating method as previously reported [29,30] and schematized in Figure 1. Samples (5 × 5 cm) were cut off from PET-CHT samples (described in the previous section) and alternately dipped during 15 min in the PCD solution (0.3% (w/v) in ultrapure water) and in the CHT solution (0.5% (w/v)) in acetic acid 1% (v/v) with intermediate drying and rinsing steps according at room temperature under

stirring (180 rpm). The weight gain after each further polyelectrolyte layer was determined following this equation.

Eq. 2: $$\textbf{Weight gain (\%)} = \frac{W_{dip\text{-}coating} - W_i}{W_i} \times 100$$

Where w_i is the weight of the virgin PET sample and $w_{dip\text{-}coating}$ is the sample weight after its modification by CHT-Gpn then followed by *n* dip-coating cycles.

The first self-assembled PCD layer adsorbed onto the CHT-Gpn primer layer (layer #1) grafted on the textile was labelled layer #2, while the following self-assembled CHT layer was labelled layer #3. So CHT layers of the system were numbered with odd values and samples terminated with 11 layers (PEM11), 15 layers (PEM15) and 21 layers (PEM21) were used as test samples. Finally, the modified textiles were cured at 140°C for 105 min to stabilize the PEM. Sample were named PET-CHT-PEMn, where n is the number of layer.

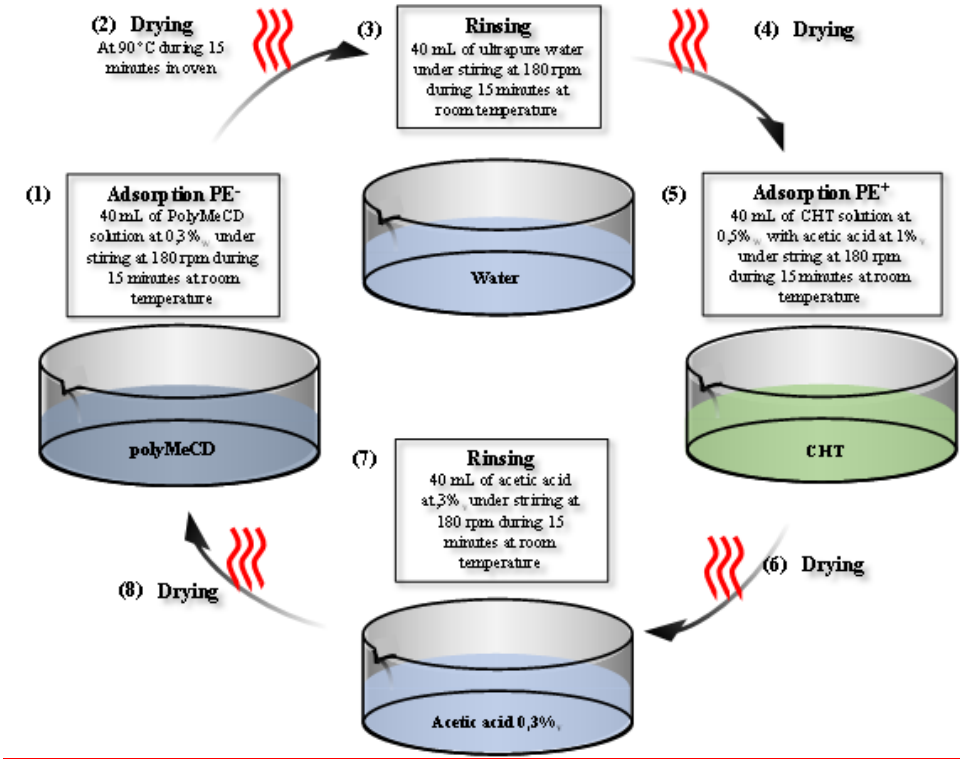


Figure 1. Schematization of the dip-coating process to build-up the multilayer system.

2.4. Textiles characterization

2.4.1. Acid orange titration

The titration of free amino group content on the textile was realized by the method described by Aubert *et al* [24]. The samples (disks of 11 mm diameter) were dipped in an orange acid (OA) solution at 2.5×10^{-2} M, pH3 at room temperature overnight under stirring (300 rpm). A calibration curve is realized preliminary with OA solution at 0.4 mM in pure water.

The amount of amino functions is calculated as follows:

Eq. 3:

$$\mathbf{NH_2,\ mmol/g} = \frac{\mathbf{Absorbance \times volume\ (L)}}{\mathbf{Slope\ (L.mol^{-1}.cm^{-1})}} \mathbf{/weight\ (g)}$$

Where "slope" is the molar extinction coefficient measured from the calibration (value = 0,014 L.mol-1.cm-1)

2.4.2. Scanning Electron Microscopy (SEM)

The SEM investigations of functionalized textiles were carried out on a Hitachi S-4700 SEM FEG (Field Emission Gun) operating with an acceleration voltage of 5–25 kV, after carbon metallization.

2.4.3. Degradation studies

The kinetics of degradation of the PEM system was performed before and after heat post-treatment at 140°C. The samples (Ø 11 mm, n = 3) are weighed (w_i) and then immersed in 10 ml of a PBS solution (37°C, 80 rpm). At regular time intervals, the samples were rinsed twice with 2 mL of ultrapure water to remove the salts adsorbed on textiles and dried at 90°C in a ventilated oven for 15 minutes. Textiles were finally weighed (w_d) and put back in fresh

PBS. The results were calculated as a percentage of the remaining mass as a function of time as follow:

Eq. 4:

$$\text{Remaining Mass (\%)} = \frac{w_d}{w_i} \text{ x } 100$$

2.4.4. In vitro biological evaluation - Cell viability

The human embryonic epithelial cell line (L132) were selected for testing the cytocompatibility of CHT functionalized textiles due to their relevance to target clinical application (skin care) and its good reproducibility. Cells were cultured in modified minimum essential medium (MEM, Gibco®, LifeTechnology) supplemented with 10% foetal calf serum (FCS, Gibco®, LifeTechnology).

After disinfection by dipping in absolute alcohol and drying at 37°C overnight, the disk samples (PET, PET-CHT, PET-CHT-PEMn) were placed in the bottom of 24-well plates (Costar, Starlab). Viton rings (Radiospare) were inserted into the wells to prevent the floating of samples, and subsequently avoid cells growing beneath the test samples. Cells were gently seeded at the density of 3500 cells cm^{-2} in each well, and the wells with no sample disk but only cell suspension served as controls, tissue culture polystyrenes (TCPS). The growth periods for the cell proliferation and cell vitality tests were 3 and 6 days without renewal of the medium.

3 and 6 days after the cell seeding, the culture medium was removed from each well and 500 µL of culture medium diluted fluorescent dye (AlamarBlue®, Interchim) was deposited in each well. After incubation at 37°C for 2 hours, the reacted dye solutions were transferred into 96-well plates (VWR International) and the non-toxic fluorescence was measured by fluorimeter (Twinkle LB970TM Berthold) at 560 nm. Data were expressed as the mean

percentage ± SD of six separate experiments with respect to the control (Tissue Culture PolyStyrene, TCPS – 100 %).

2.5. Textiles loading with chlorhexidine

2.5.1. CHX quantification

High-Performance Liquid Chromatography (HPLC) coupled to UV detection (HPLC-UV) (Shimadzu LC-2010A-HT, Shimadzu, Japan) was used according to the method described by Xue *et al* and Kudo *et al* to analyse the CHX [35,36]. The analysed solutions containing CHX were separated with a reverse-phase column (C18-MG, 5 µm, 110 Å, 250×46mm, Phenomenex Gemini) maintained at 40°C. The mobile phase consisted of acetonitrile/water (40:60) containing 0.05% (v/v) trifluoroacetic acid, 0.05% (v/v) heptafluorobutyric acid and 0.1% (v/v) triethylamine. The flow-rate was 1 ml/min and the injection volume 10 µl. CHX was detected at 260 nm with a retention time of 6-7 min.

2.5.2. CHX phase solubility diagram

Phase solubility studies were carried out according to the method described by Higushi and Connors [37]. Excess amount of CHX was added to MeβCD and MeβCD polymer (PCD) solutions in water at different concentrations ranging from 0 to 80 mM in CD cavities. The mixtures were shaken (120 rpm, room temperature) for 24h and filtered through a 0.45µm membrane filter. The concentration of CHX in the supernatant was determined with the HPLC method previously described. Phase solubility diagrams were obtained by plotting the solubility of CHX in mmol/L versus CD concentration in mmol/L. According to [38], association constant (K_a) value of CD/CHX inclusion complex was calculated from the slope of the linear part of the phase–solubility diagrams using the following equation:

Eq. 5:

$$K_a = Slope / (S_0 *(1-Slope))$$

Where S_0 is the intrinsic solubility of CHX in the absence of CD and *Slope* is the slope of the linear part of the phase–solubility profile.

The solubilizing power of CD was evaluated by the complexation efficiency (CE) parameter. CE is the complex to free CD concentrations ratio and was calculated from the slope of the phase solubility diagram:

Eq. 6:

$$CE = S_0 * K_a = [CD\text{-}CHX] / [CD] = Slope / (1\text{-}Slope)$$

Where [CD-CHX] is the concentration of dissolved inclusion complex and [CD] is the concentration of free CD.

2.5.3. CHX loading and release kinetics

Drug Loading - Textile samples (∅ 11mm) were impregnated in a saturated aqueous suspension of CHX (0.4 mg/mL) under stirring (210 rpm) overnight at room temperature. The samples were briefly rinsed with ultrapure water, dried and stored at 37°C before evaluation.

Sorption capacities of textiles were measured by immersion of samples (∅ 11 mm) in 15 ml of NaOH (0.5 M) under sonication for 1 hour and then under stirring (300 rpm) for 24 hours. The pH of supernatant solutions (n=6) were adjusted to 4 with acetic acid (50% (v/v)) and CHX was quantified by HPLC.

CHX release kinetic - Loaded samples (∅ 11mm) were placed in 24 well-plate (CytoOne®) containing 1 mL of PBS solution under 80 rpm at 37°C. At predetermined intervals (30 minutes – 37 days), the release medium was completely removed and replaced with fresh PBS. The CHX content in the release medium (n=6) was determined by HPLC. Release medium and sample were stored at 37°C for microbiological evaluation.

2.5.4. In vitro microbiological evaluation

Microbiological tests were performed according to the standardized Kirby–Bauer method [39]. 50 µL of the release medium were placed in wells in Mueller Hinton agar plates pre-inoculated with *Staphylococcus aureus* (*S. aureus*, CIP224) strains. After 24 h of incubation (37°C), the inhibition zone was measured. The values were plotted as a function of the soaking time in PBS to evaluate the antimicrobial activity of the disk sample and release medium (n=6)

3. Results and discussion

3.1. PET modification with CHT-Gpn

3.1.1. Influence of CHT concentration and reaction time

CHT immobilization on PET through crosslinking reaction with Gpn could be observed thanks to parallel weight gain and amino groups assessments after washing samples with diluted acetic acid. Figure 2 shows the parallel evolution of the weight gain and the amino groups content on the textile in function of the time of crosslinking for PET samples impregnated and roll-padded in CHT solutions (1.0% and 2.5% (w/v)) containing Gpn at concentration fixed to 0.1%w/v. For the highest concentration of CHT (2.5% (w/v)), the weight gain and the amount of amino groups rapidly increased and reached a plateau value at 24 hours with a maximum of 1.9%-wt and 0.15 $mmol.g^{-1}$ respectively. For the lower concentration of CHT (1% (w/v), the crosslinking reaction could be detected by both characterization techniques only from 8 hours of reaction. A maximum value was reached after 24 hours, with a weight gain and amino content of 0.68%$_w$ and 0.06 $mmol.g^{-1}$ respectively. For both parameters, the degree of functionalization was 2.8 times higher in 2.5%w/v compared to 1%w/v CHT solutions, so that a linear response was observed. CHT crosslinking reaction by Gpn is produced by the nucleophilic substitution of the ester function of Gpn by the primary amine group of CHT to form a secondary amide and also by the nucleophilic attack on the dihydropyran group of Gpn by the primary amine of CHT resulting in the formation of a six membered nitrogen heterocycle [26]. Besides, the self-polymerization of Gpn forming chromophore groups absorbing at 605 nm induced the progressive blue dyeing of the textiles. This observation is in accordance with the different studies on the crosslinking evaluation of CHT by Gpn both in term of reaction time (24 hours) than in the blue coloration in studies dealing with CHT hydrogels [40], matrices [41] or nanofibers [19] crosslinked by Gpn. According to the reaction kinetic study, we opted for

applying a CHT concentration of 2.5% (w/v) for 24 hours as optimal conditions to obtain a maximum and repeatable yield of functionalization on the textiles.

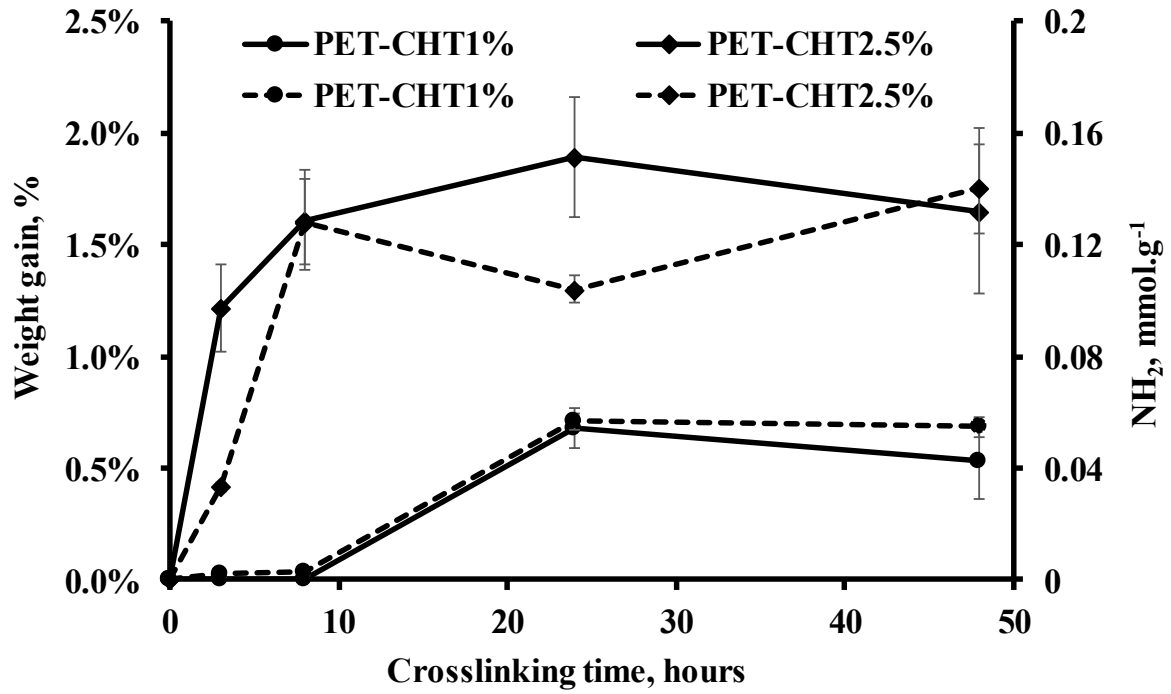


Figure 2: Weight gain (solid line) and of the amino groups (-NH_2) (dashed line) contents in mmol/g of the PET textile functionalized with CHT (concentrations 1% and 2.5% (w/v)) reticulated with Gpn (concentration 0.1% (w/v) in function of the reaction time at 25°C.

3.1.2. Influence of the concentration of Gpn

Samples were impregnated in CHT solutions whose concentration was fixed to 2.5%w/v) and Gpn in variable concentrations from 0.01 up to 0.5%w/v, roll-padded and left in the humid ambiance at 25°C for 24 hours. Figure 3 shows that the weight gain increased from 0.2%-wt up to 1.4%-wt when Gpn increased from 0.05 to 0.1%w/v. It is worth mentioning that in absence of Gpn, CHT was completely removed during the washing step. The amount of amino groups determined by spectrophotometry increased with the Gpn concentrations and reached an optimal value (0.1 mmol/g) for Gpn concentration of 0.1%

(w/v). Besides, the blue dyeing of the textile significantly appeared after the 24 hours period of exposure in moist ambience at Gpn concentration higher than 0.1% (w/v). Despite their highest weight increase, samples reticulated in presence of 0.5%w/v Gpn displayed amino groups content in the same range of order as those prepared from 0.1% Gpn. This was probably due to a surface saturation phenomenon that involved the stabilization of the surface density of amino groups accessible to acid orange dye.

According to these results, we opted for applying a Gpn concentration of 0.1% (w/v) as the best compromise with regard to the resulting weight gain (1.0%wt) and amino groups density (0.1 mmol/g) on the PET-CHT supports. This support called PET-CHT presented a cationic surface (after protonation of CHT amino groups) that was used for the build-up of the PEM system as described in the next section.

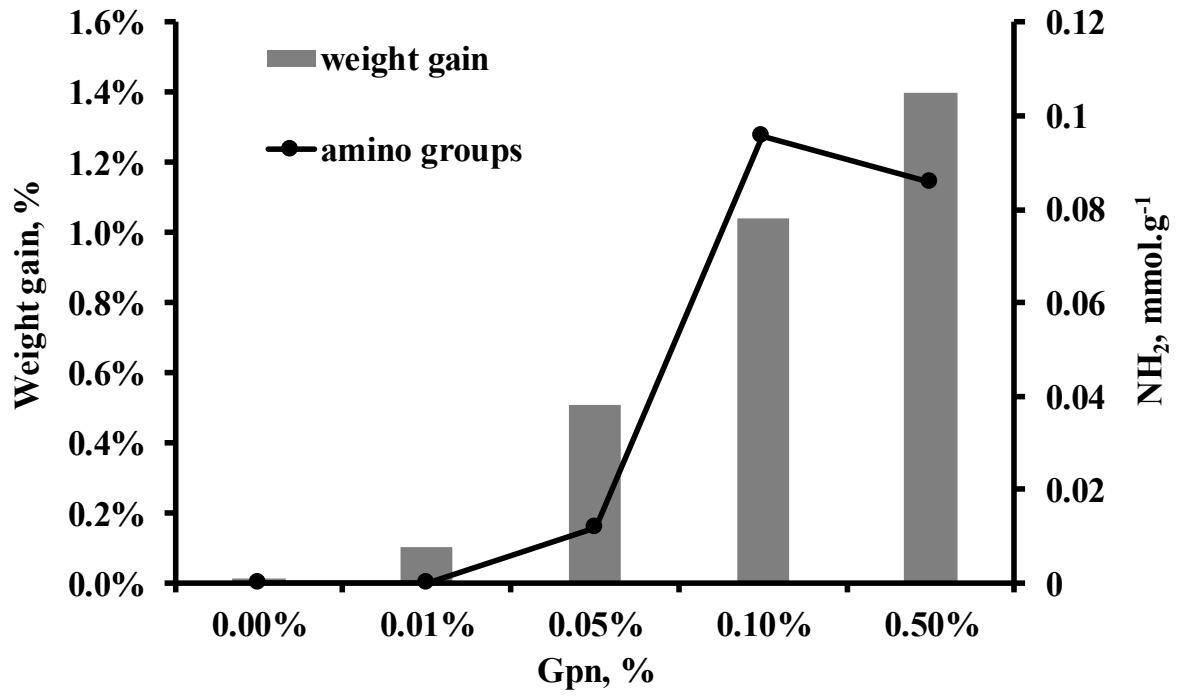


Figure 3: Influence of the concentration of the crosslinking agent (Gpn, 25°C, 24 hours) on the weight gain and on amino groups content (mmol/g) of the PET textile. The concentration of CHT was fixed to 2.5% (w/v) and the reaction time was 24 hours.

3.2. Build-up of the polyelectrolyte multilayer system (PEM) on PET-CHT

Figure 4 reports the weight gain of PET samples after the preliminary CHT immobilization with Gpn (PET-CHT sample) and in the course of the subsequent cycles of the dip-coating process. The polyelectrolyte complex formation through electrostatic interactions between ammonium groups of CHT crosslinked by Gpn on PET-CHT surface (layer #1) and the carboxylate groups of the water-soluble anionic CD polymer occurred and induced the first PCD layer deposition (layer #2). By a phenomenon of charge overcompensation, the surface acquired an anionic charge available for the self-assembly of the next CHT layer (layer #3) and this was repeated in order to build-up a L*b*L coating made of up to 21 layers.

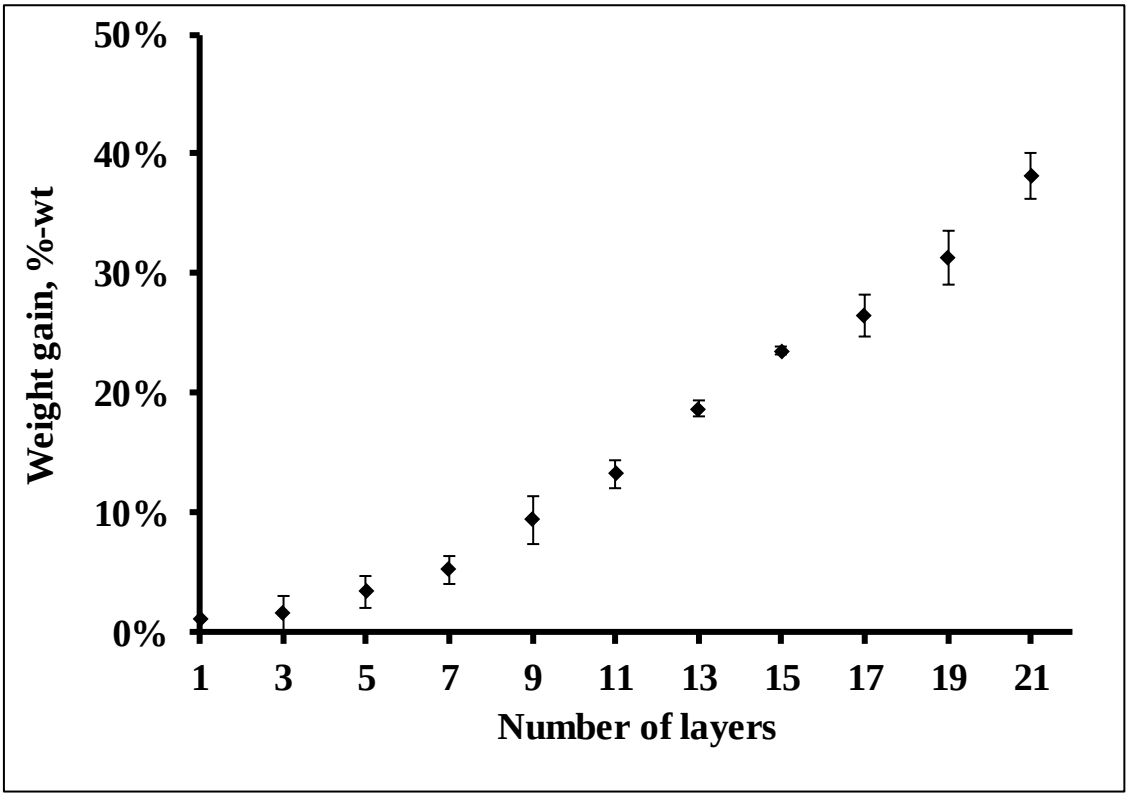


Figure 4: Weight gain (in %-wt) of the PET textile with the number of CHT layers. Layer#1 corresponds to the CHT layer reticulated with Gpn. The following odd numbered layers correspond to self-assembled CHT layers alternately deposited with PCD layers. PCD and CHT concentrations used in the dip coating process were 0.3%w/v and 0.5% w/v respectively

As observed in Figure 4, the growth profile of the LbL assembled multilayer consists of an exponential followed by a linear part that is classically reported in similar studies. In the present case, the transition between both exponential and linear regimes (called the *switch point*) [42] occurs after the fifth CHT layer deposition (3.37%wt) and then a linear evolution of the weight gain reached up to 38.13%wt (21 layers) ($r^2 = 0.9943$). The exponential part can be explained by the coalescence of initially formed islands of polyelectrolytes on the fibres surface that progressively leads to homogeneous coating. Once the available surface is covered and if polyelectrolytes are not able to diffuse into the multilayer system, a linear growth of the film is then observed [43–46].

3.2.1. PEM stabilization by heat post-treatment

Once dipped in saline solutions, PEM assemblies present more or less rapid degradation due to the dissociation of the polyelectrolyte complexes involved by the competing ionic species from the solution. ~~Such phenomenon is currently reported in the literature, and in our previous works. For example, Martin et al (2013b) [30] displayed degradation in PBS buffer at pH 7.4 within 4 days of a similar PEM system based on CHT and PCD~~. To circumvent this, we previously successfully applied ~~a~~ a thermal treatment at 140°C to a similar PEM system based on CHT and PCD [30] on the one hand, and on CHT-PCD based nanofibers on the other hand [47]. ~~Such strategy was recently successfully applied by our group on electrospun nanofibers based on CHT and PCD polyeletrolyte complexes. As a matter of fact, we could observe that a thermal treatment at 140°C markedly improved the stability of nanofibers over a period of two weeks in pH5.5 buffered solution while nanofibers without thermal treatment were readily solubilized in such acidic medium~~. We could evidence that such thermal post treatment provoked the crosslinking of the polyelectrolyte complex through amide groups formation from carboxylic groups of PCD and amino groups of CHT [47] ~~as displayed in figure 5A~~.

~~Therefore, applying the same strategy to the PEM coating was expected to provide the same crosslinking reaction between CHT and PCD layers as schematized in Figure 5A~~. This crosslinking reaction was confirmed by titrating the amino functions on PET-CHT-PEMn samples before and after the thermal post-treatment (TT) (Figure 5B). Indeed, before the thermal treatment, the density of amino functions considerably increased after PEM build-up [325 to 350 nmol.g^{-1}] compared to PET-CHT [95.8 nmol.g^{-1}]. Unlike what was observed for the PET-CHT sample, the thermal treatment of samples modified with the LbL film provoked a significant decrease of amino functions. This confirmed our hypothesis of the partial conversion of both some amino groups of CHT layers and some carboxylic acid groups of CD layers into amide bonds resulting in the stabilization of the L*b*L assembly.

It is worth mentioning that a ATR-FTIR study was carried out in order to evidence 1) L*b*L build-up on the PET support, and 2) the formation of amide groups induced by thermal post-treatment. However as displayed in supplementary data (Figure S1), except a new band corresponding to C-O-C vibration in polysaccharides at 1038 cm^{-1} appearing on spectra of treated samples, the fingerprint of PET masked most of the expected signals due to L*b*L deposition.

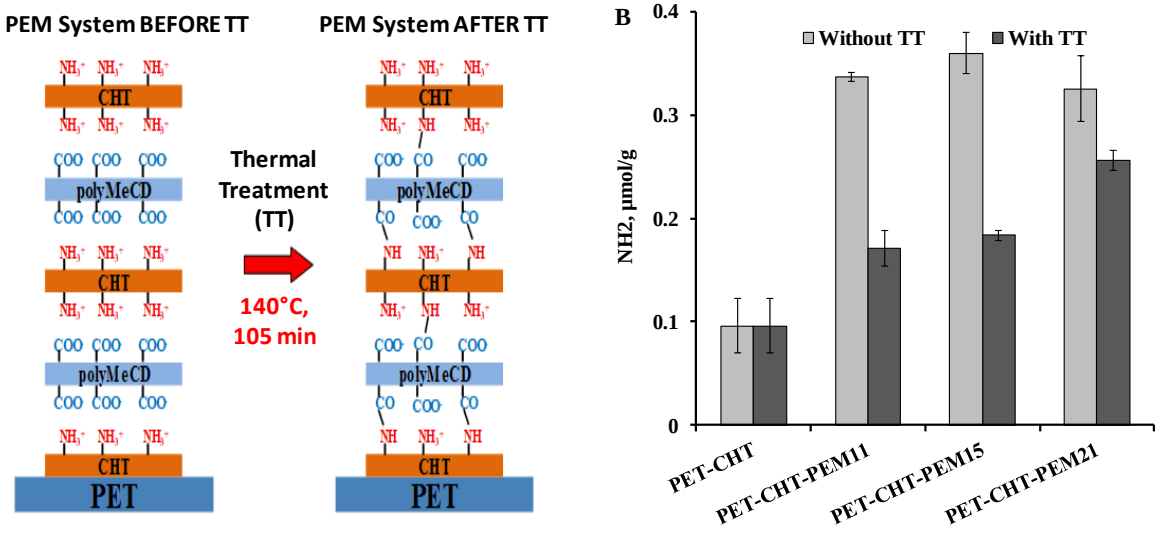


Figure 5: (A) Scheme of the formation of amide bond within the PEM system during heat treatment (140°C - 1h45). (B) Amino groups content of PET textiles modified with CHT crosslinked with Gpn and coated with PEM films based on 11, 15 and 21 CHT layers before and after thermal post treatment (TT) at 140°C during 105 min.

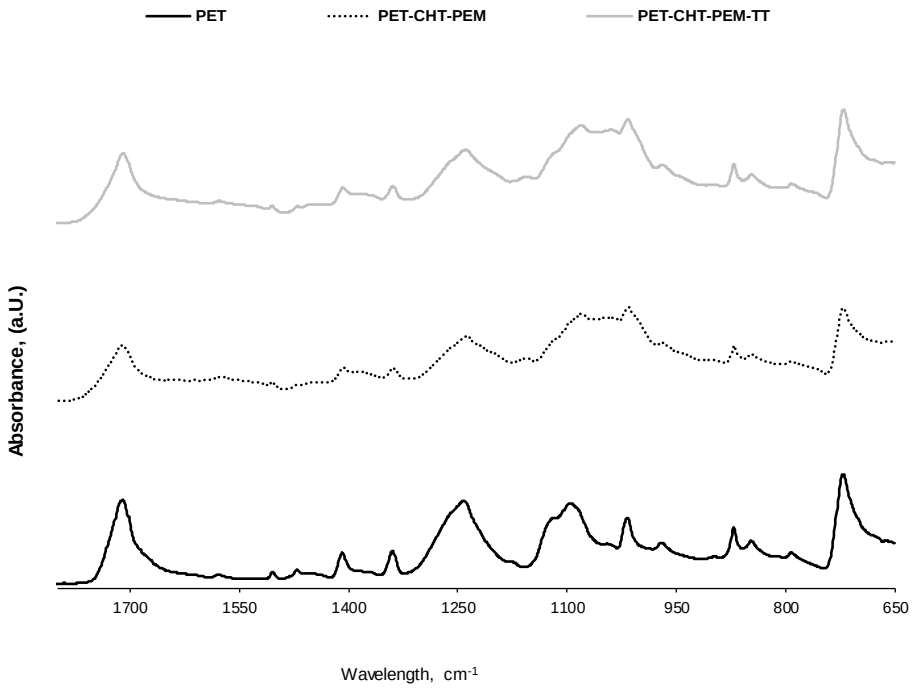


Figure S1: FTIR spectra for the different stage of functionalisation, i.e. PET, PET with multilayer system (PET-CHT-PEM) and PET with multi-Layer System (PET-CHT-PEM-TT).

3.3. Scanning Electron Microscopy

Textile surfaces at different stages of their conception were analyzed by scanning electron microscopy (Figure 6). The virgin PET fibres are smooth, spaces between fibers form open pores, and some fibres are slightly deformed or welded due to the textile manufacturing process by heat setting. PET-CHT reveals the presence of CHT visible especially at the crossings of the fibres, but does not appear obviously due to the spreading of CHT coating forming a thin film corresponding to 1.0% of the total weight of the material at this step of the

process. When the multilayer system is applied, the coverage of the textile fibres by the PEM coating can be clearly observed, as well as the pores close-up. Despite the fibers coating and porosity filling by CHT-PCD polyelectrolyte complex, only a moderate stiffening of the treated textiles was noticed, even in case of PEM 21 sample.

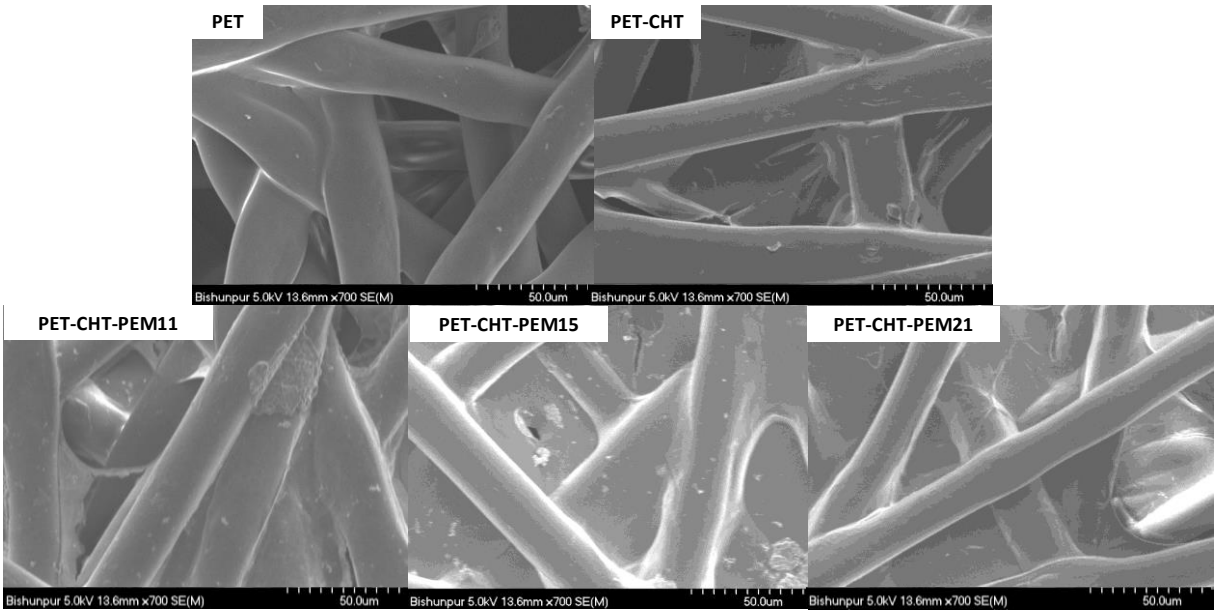
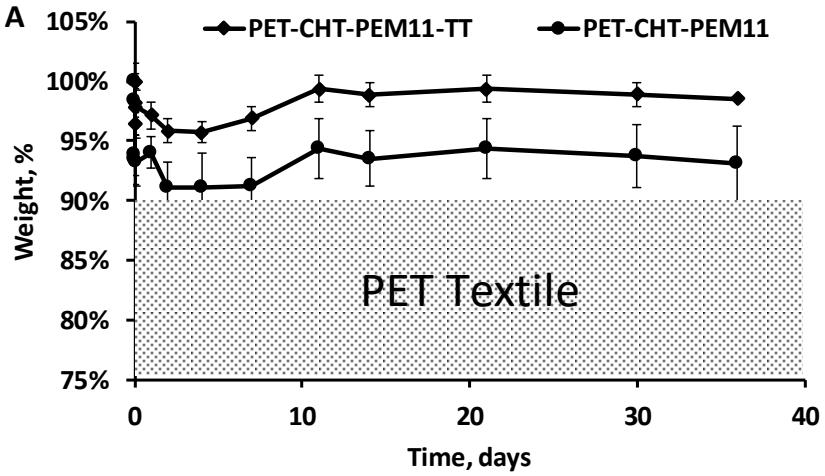


Figure 6: SEM micrographs obtained by scanning electron microscopy of samples at different stages of the process, virgin PET, PET modified by Gnp crosslinked CHT, and after PEM deposition up to 11, 15 and 21 CHT layers.

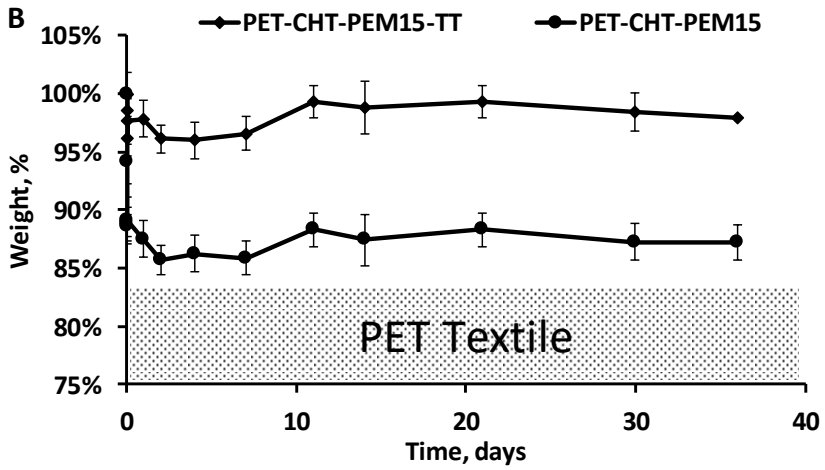
3.4. *In vitro* degradation studies

Figure 7 shows the evolution of the weight of the multilayer system as a function of the degradation time in PBS medium. No significant degradation was observed for PET- CHT samples after 5 weeks in PBS, confirming the stability of the first layer of CHT immobilized on PET by crosslinking with Gpn. On the other hand, PEM self-assembled systems without thermal post treatment revealed a rapid and significant degradation after 3 days in the PBS solution. Thus, PEM11; PEM15 and PEM21 lost 10%, 15% and 20% of their initial weights respectively, corresponding to the totality of the PEM coating for each of the samples. Conversely, heat-treated PEM systems displayed degradations values inferior to 5%. This

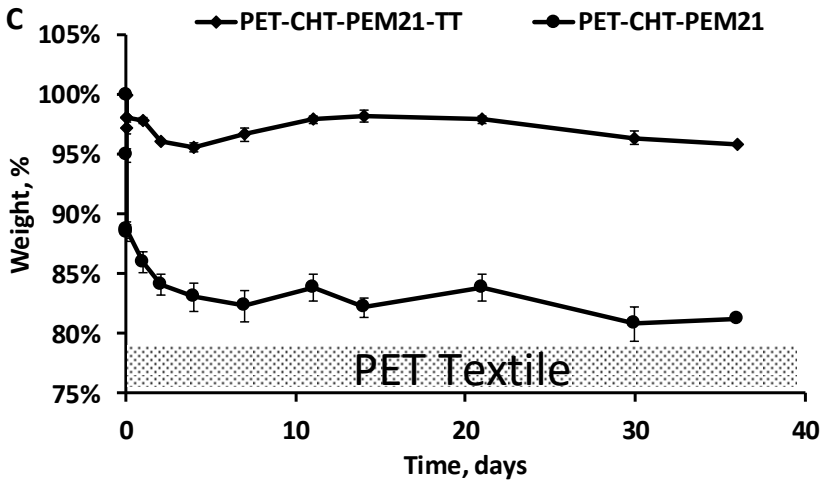
409 result confirms is an indirect evidence of the crosslinking of the LbL coating upon heating as
410 discussed previously.



411



412



413

414 *Figure 7: Weight (%w) of the PEMn samples (n= 11; 15; 21) systems with or without thermal*

415 *treatment (TT) in function of the time of degradation in PBS (37°C, 80 rpm)..*

416

3.5. *In vitro* biological evaluation

The cytocompatibility of the textiles was evaluated with epithelial cells line L132 (ATTC-CCL5), for their high sensibility with toxic products according to ISO 10993-5. Cells were seeded onto the different textiles: PET, PET- CHT-Gpn, PEMn samples with or without TT.

Figure 8 confirms the cytocompatibility of PET support which remained unchanged after coating with crosslinked CHT by Gpn, 99.0% and 104.4% respectively, after 3 days of incubation. This result is in agreement with the work of Li et al. and Lau et al. who showed the good cytocompatibility of electrospun CHT membranes crosslinked with Gpn in contact with purified Schwann cells and fibroblasts (L929) [19,48].

Nevertheless, Figure 8 also displays that samples coated with PEM provoked a decrease of cell vitality when increasing the number of layers from PEM15 to PEM21. Besides, in a former study from our group, Martin et al (2013b) [30] observed the same phenomenon explained by the release of PCD in the culture medium that provoked the pH decrease and cell death. Our results display that heat treatment applied to PEM samples improved their cytocompatibility due to crosslinking reactions between PCD and CHT that prevented the above mentioned phenomena. Furthermore, the lower cell proliferation on PEM system compared to PET-CHT can also be explained by a low initial adhesion of the cells on the coating surface. Indeed, Muzzio et al also showed that cell adhesion decreased when thermal treatment was applied to the multilayer system [49].

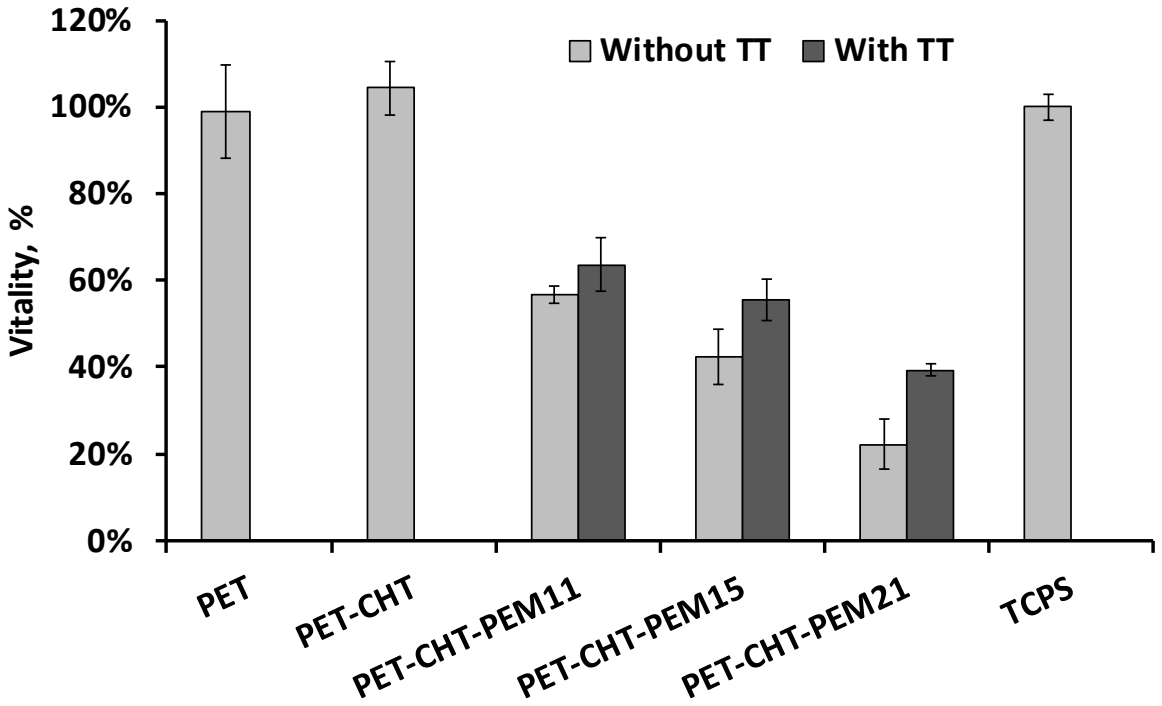


Figure 8 : Cell vitality (Alamar Blue method) of L132 cells on PET, PET-CHT and PET-CHT-PEMn samples (n = 11; 15; 21) with or without thermal post treatment (140°C, 1:45h) after 3 days of culture (37°C, 5% CO_2, 100% RH), without renewal of the culture medium (n=6).

3.6. Drug sorption and Drug release

3.6.1. Solubility Diagram of CHX

Solubility enhancement studies of CHX in presence of MeβCD and MeβCD polymer (PCD) were carried out using the phase solubility method (Figure 9). CHX solubility linearly increased with MeβCD (r^2=0.987) and PCD (r^2=0.994) concentration, displaying in all cases AL-type profiles. Inclusion complexes of CHX with MeβCD and PCD[50] were evidenced by an association constant respectively of 640 M^{-1} and 820 M^{-1}. S_0 of CHX in water at room temperature was = 0.15 mM ± 0.015 mM while a maximum of 6.87 mM ± 0.25 mM was obtained in presence of 62.1 mM of PCD. So PCD increased remarkably the solubility of

CHX by a factor 50. This result can be explained by the crosslinked macromolecular structure of PCD interacting with the aromatic groups of CHX through *host-guest* interactions with neighboring CD cavities on the one hand, and through ionic interactions between cationic biguanidinium groups of CHX and free carboxylate groups carried by the citrate groups crosslinks [51,52].

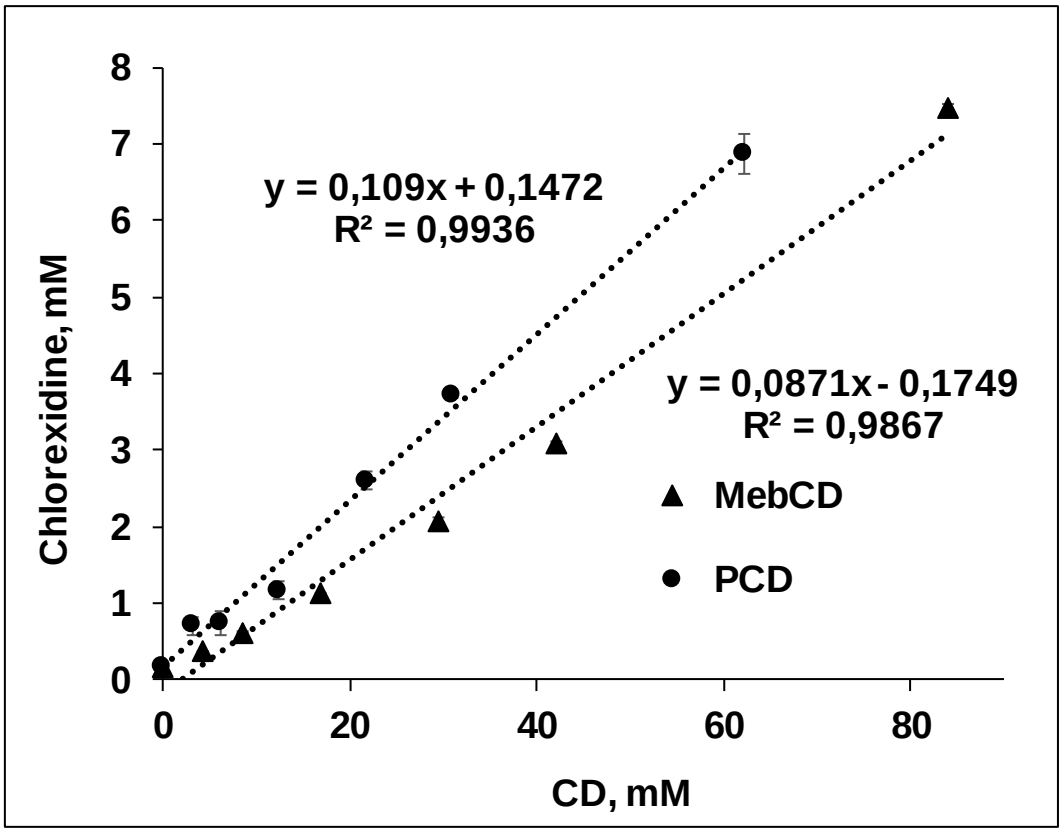


Figure 9: Solubility diagram of CHX with increasing concentrations of MeβCD and MeβCD polymer (PCD) in aqueous solution at room temperature after 24 hours of stirring (240 rpm). S_0 =0.15 +/- 0.015 mmol/L at room temperature

3.6.2. CHX Loading on PEM samples

Textile samples were impregnated in CHX 0.4 mg/mL aqueous solutions (Figure 10). It clearly appears that PEM samples could adsorb CHX on the contrary of virgin PET and PET-CHT samples. These results highlight the crucial role played by PCD in the CHX loading. In addition, increasing the number of layers in the PEM system emphasizes this phenomenon.

Thus, the amount of adsorbed CHX increased with the number of layers from 45.1 mg/g (PEM11) up to 143.7 mg/g (PEM21). However, PEM samples after heat treatment displayed reduced CHX uptakes compared to untreated ones. Furthermore, CHX uptake in this case was no related to the number of layers. This can be explained by the crosslinking of the PEM, which limits its swelling, and therefore CHX diffusion into the LbL coating. Elsewhere, Diamanti et al. (2016) [53] have shown that a heat treatment applied to a multilayer system reduced significantly the wettability of the surface (water contact angle 36° vs 95° with TT (145°C))

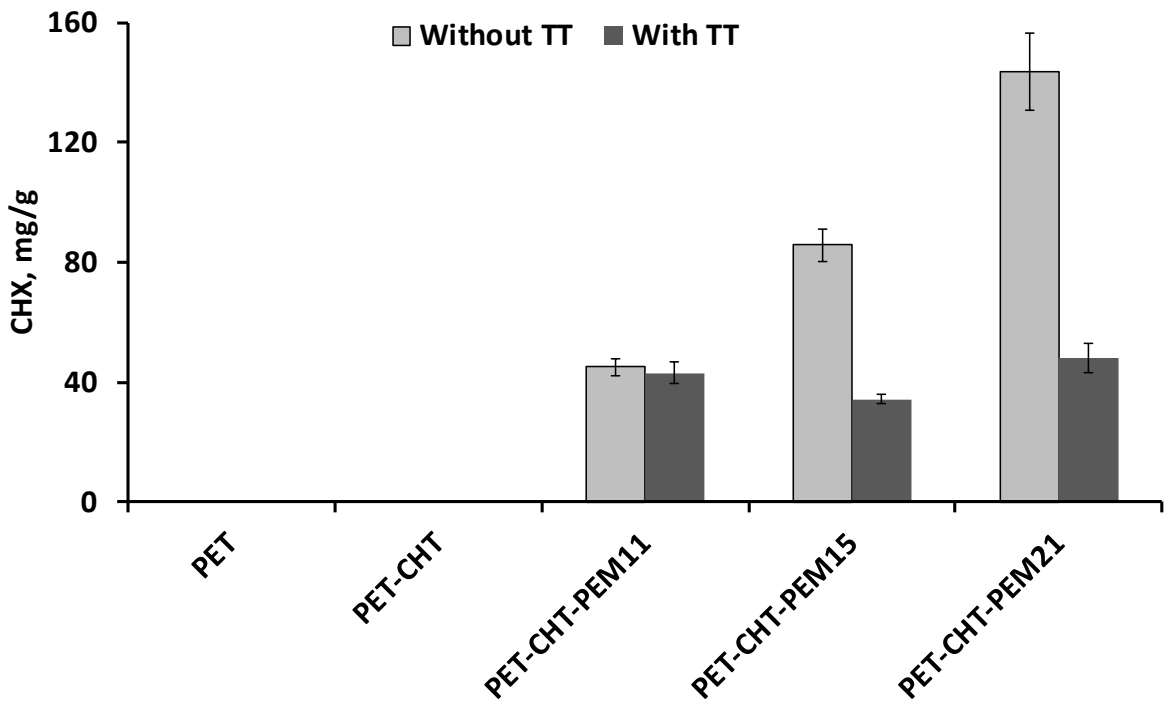


Figure 10 : CHX adsorbed onto PET, PET-CHT and PET-CHT-PEMn samples (n= 11; 15; 21) with or without thermal treatment. Textile samples are impregnated in CHX solution (0.4 mg/ml) overnight. Loaded textiles are desorbed in NaOH solution (0.5M, 4 hours).

3.6.3. CHX release from PEM samples

Interestingly, Figure 12A shows that the number of layers applied to the textile has an impact on i) the percentage of CHX immediately released (Burst effect), ii) the percentage of CHX delivered over time and iii) the release time.

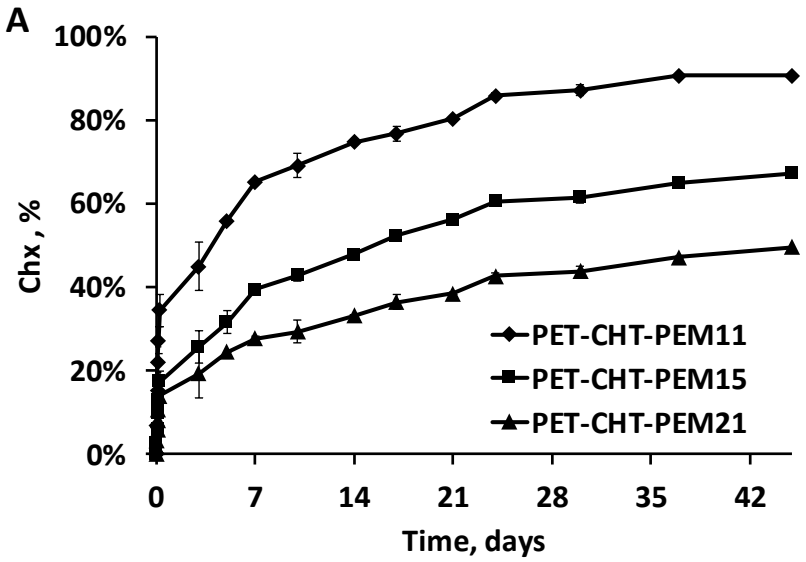
As a matter of fact, Figure 11 displays the sudden release of CHX from all PEM samples within the first instants of the release test. The extension of this burst release was related to the number of layers in orders PEM11> PEM15>PEM21, corresponding to 34%, 17%, 13%, and 47%, 24% and 8% before and after thermal treatment respectively. This fast release step can be explained by the liberation of CHX in interaction with the LbL coating through weak and non-specific interactions with the polyelectrolytes (hydrogen and electrostatic bondings). After the burst release, delayed release of CHX was observed in a second phase where the influence of thermal treatment on the release profile is observed. As a matter of fact, in case of PEM samples without thermal treatment the decreasing of slope of the curves against time of release reveals that the delivered dose decreased with time up to 45 days. On contrary, concerning thermally treated samples, an almost linear release profile was observed, synonym of a constant rate of delivery within the whole period of the experiment.

Finally, Figure 11 also displays the influence of the number of layers on the overall released CHX dose within the 45 days period for samples before (Figure 11A) and after (Figure 11B) thermal treatment. As a matter of fact, after 45 days, 91, 67 and 50% of loaded CHX were released from PEM11, PEM15 and PEM21, respectively and these values decreased down to 68, 50 and 33% after thermal treatment.

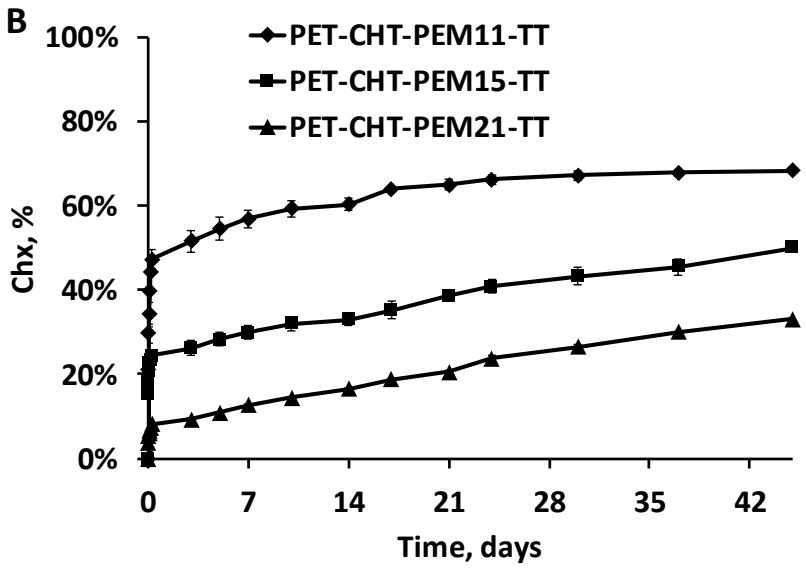
In conclusion, the release of CHX could be controlled not only by the number of layers but also by the application of a thermal treatment. Firstly, the number of layers controls coating thickness in the PEM system. If thickness increases, the percentage of drug released decrease and the release is prolonged. In relation to Figure 7, the release is initially controlled

503 by degradation phenomenon resulting in a burst effect, then by a diffusion / degradation
504 phenomenon with the remaining layers of polyelectrolytes on the textile. Secondly, the release
505 is also controlled by the inclusion of CHX inside the cavities of CDs as shown on cellulose
506 functionalized with CDs [51,54].

507 Thirdly, as observed in Figure 12B, the release profile is also controlled by the
508 crosslinking of the PEM system upon heat treatment. Interestingly, the thermal treatment
509 contributed to slow down the release rate of the CHX in function of the number of layers
510 applied to the textile. Indeed, after 45 days, the PET-CHT-PEM21 system released 40% of the
511 CHX while the thermal-treated system released only 25%.



512



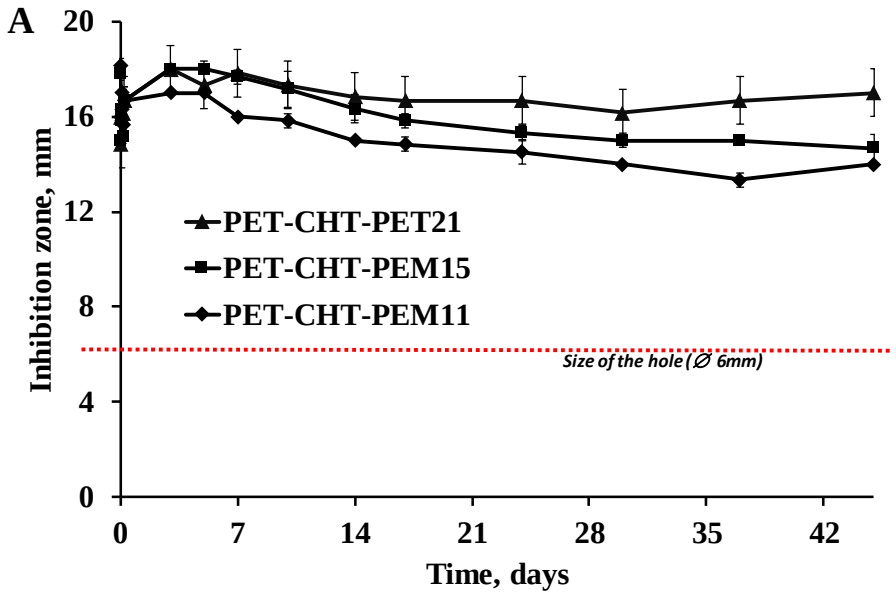
513

514 Figure 11. In batch CHX release in PBS (pH 7.4, 80 rpm, 37°C) from PET-CHT-PEMn
515 samples (n = 11; 15; 21) without (A) and with (B) thermal treatment (total medium renewal at
516 each time point). Textile samples were preliminarily impregnated in CHX solution (0.4
517 mg/ml) overnight.

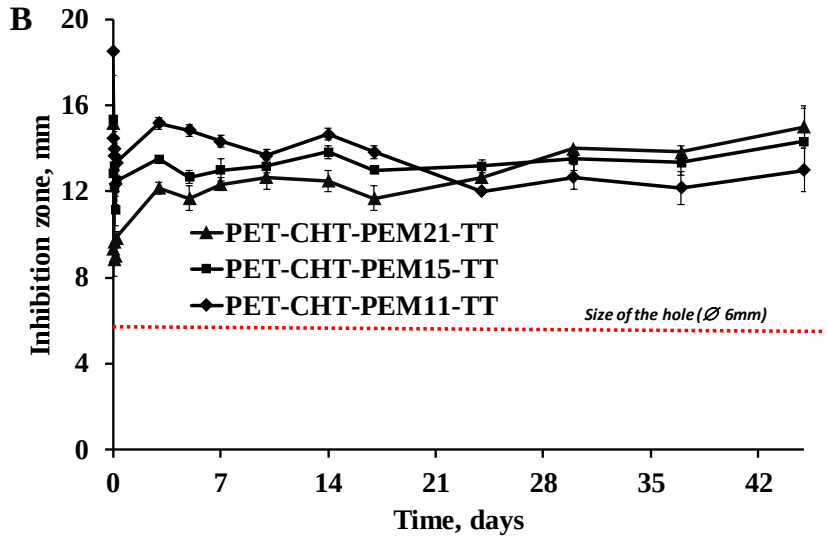
518 ***3.6.4. Antibacterial activity***

519 The antibacterial effect against *S. aureus* of aliquots withdrawn from release medium (PBS
520 (pH 7.4, 37°C, 80 rpm) is plotted against time in Figure 12. The inhibition zone size varied
521 with the contact time, the number of self-assembled layers applied on the textile, and with the
522 application of the thermal treatment. Firstly, an overview of Figure 12 revealed that the
523 antibacterial activity of the release media persisted along the 45 days period of the assay.
524 Nevertheless, Figure 12A shows the diameter of the zone of inhibition is increased with the
525 number of layers applied on the textile in relation to the release profile obtained in Figure 11.
526 Indeed, the amount of CHX release increased with the number of layers. Figure 12B also
527 shows the impact of the number of layers on antibacterial activity. Interestingly, whatever the
528 release time and the number of layers, the diameter of the zone of inhibition is lower than that
529 observed for the same textiles without thermal treatment. This also confirmed the results

obtained in terms of release. Indeed, the amount of CHX released is lower for thermally treated textiles compared to untreated ones. Finally, the number of layers applied to the textile and the thermal post treatment could control the release of the CHX while having antibacterial activity until 45 days.



536



537

538 Figure 12. Evolution of the antimicrobial activity against *S. aureus* of release medium from
539 PET-CHT-PEMn with or without thermal treatment in PBS (pH 7.4, 80 rpm, 37°C) with total
540 renewal medium at each time. Textile sample are impregnated in CHX solution (0.4 mg/ml)
541 overnight.

542 **4. Conclusion**

543 In this paper, we report the surface modification of a polyester nonwoven textile with CHT
544 crosslinked in mild conditions using Gpn. The resulting surface cationic charge density was
545 controlled by the reaction time and the concentration of the reagents (CHT and Gpn). A

textile treatment with a 2.5% CHT solution cross-linked with 0.1% Gpn for 24 hours seems to be a good compromise to obtain an optimal amino function density for the construction of a PEM system while cytocompatibility was of the support was preserved.

Then, a layer-by-layer coating based on PCD and CHT was built-up resulting in the enhanced reservoir capacity and sustained release of CHX depending of the number of layers. Nevertheless, a rapid degradation of the multilayer system has been observed. In a very interesting way, a compromise was found by applying a thermal post-treatment to stabilize the multilayer system and to control the release of the drug over several weeks. Despite this thermal treatment reduced the drug loading capacity (especially for the highest number of layers) it allowed to maintain eventhough an antibacterial activity up to 7 weeks. Furthermore, thermal post-treatment also enhanced the cytocoamptibility of the PEM system. In addition, the antibacterial activity *in vitro* over several weeks has been demonstrated on two strains (E. coli and S. aureus). *In vivo* tests still have to be performed in a next future in order to display the efficiency of such modified textiles as wound dressings, and open the way to other types of biomedical textiles for the prevention of infections.

Acknowledgment

This research was funded by FONDECYT-CONCYTEC (grant contract number 238-2015-FONDECYT)

References

[1] M.A. Fonder, G.S. Lazarus, D.A. Cowan, B. Aronson-Cook, A.R. Kohli, A.J. Mamelak, Treating the chronic wound: A practical approach to the care of nonhealing wounds and wound care dressings, J. Am. Acad. Dermatol. 58 (2008) 185–206. doi:10.1016/j.jaad.2007.08.048.

[2] V.T.M. Le, C. Tkaczyk, S. Chau, R.L. Rao, E.C. Dip, E.P. Pereira-Franchi, L. Cheng, S. Lee, H. Koelkebeck, J.J. Hilliard, X.Q. Yu, V. Datta, V. Nguyen, W. Weiss, L. Prokai, T. O'Day, C.K. Stover, B.R. Sellman, B.A. Diep, Critical Role of Alpha-Toxin and Protective Effects of Its Neutralization by a Human Antibody in Acute Bacterial Skin and Skin Structure Infections, Antimicrob. Agents Chemother. 60 (2016) 5640–5648. doi:10.1128/AAC.00710-16.

[3] Z. Song, H. Sun, Y. Yang, H. Jing, L. Yang, Y. Tong, C. Wei, Z. Wang, Q. Zou, H. Zeng, Enhanced efficacy and anti-biofilm activity of novel nanoemulsions against skin burn wound multi-drug resistant MRSA infections, Nanomedicine Nanotechnol. Biol. Med. 12 (2016) 1543–1555. doi:10.1016/j.nano.2016.01.015.

[4] Y. Gao, R. Cranston, Recent Advances in Antimicrobial Treatments of Textiles, Text. Res. J. 78 (2008) 60–72. doi:10.1177/0040517507082332.

[5] P. Gupta, S. Chhibber, K. Harjai, Efficacy of purified lactonase and ciprofloxacin in preventing systemic spread of Pseudomonas aeruginosa in murine burn wound model, Burns J. Int. Soc. Burn Inj. 41 (2015) 153–162. doi:10.1016/j.burns.2014.06.009.

[6] A.K. Gupta, P. Batra, P. Mathur, A. Karoung, B.T. Thanbuana, S. Thomas, M. Balamurugan, J. Gunjiyal, M.C. Misra, Microbial epidemiology and antimicrobial susceptibility profile of wound infections in out-patients at a level 1 trauma centre, J. Patient Saf. Infect. Control. 3 (2015) 126–129. doi:10.1016/j.jpsic.2015.06.001.

[7] J.M. Schierholz, J. Beuth, Implant infections: a haven for opportunistic bacteria, J. Hosp. Infect. 49 (2001) 87–93. doi:10.1053/jhin.2001.1052.

[8] K.K. Chung, J.F. Schumacher, E.M. Sampson, R.A. Burne, P.J. Antonelli, A.B. Brennan, Impact of engineered surface microtopography on biofilm formation of Staphylococcus aureus, Biointerphases. 2 (2007) 89–94. doi:10.1116/1.2751405.

[9] P.H.S. Kwakman, A.A. te Velde, C.M.J.E. Vandenbroucke-Grauls, S.J.H. van Deventer, S.A.J. Zaat, Treatment and prevention of Staphylococcus epidermidis experimental biomaterial-associated infection by bactericidal peptide 2, Antimicrob. Agents Chemother. 50 (2006) 3977–3983. doi:10.1128/AAC.00575-06.

[10] B.S. Nagoba, B.J. Wadher, A.K. Rao, G.D. Kore, A.V. Gomashe, A.B. Ingle, A simple and effective approach for the treatment of chronic wound infections caused by multiple antibiotic resistant Escherichia coli, J. Hosp. Infect. 69 (2008) 177–180.

612 doi:10.1016/j.jhin.2008.03.014.
613
614 [11] M. van de Lagemaat, A. Grotenhuis, B. van de Belt-Gritter, S. Roest, T.J.A.
615 Loontjens, H.J. Busscher, H.C. van der Mei, Y. Ren, Comparison of methods to evaluate
616 bacterial contact-killing materials, Acta Biomater. 59 (2017) 139–147.
617 doi:10.1016/j.actbio.2017.06.042.
618
619 [12] V. Ambrogi, D. Pietrella, M. Nocchetti, S. Casagrande, V. Moretti, S. De
620 Marco, M. Ricci, Montmorillonite–chitosan–chlorhexidine composite films with antibiofilm
621 activity and improved cytotoxicity for wound dressing, J. Colloid Interface Sci. 491 (2017)
622 265–272. doi:10.1016/j.jcis.2016.12.058.
623
624 [13] S.S.D. Kumar, N.K. Rajendran, N.N. Houreld, H. Abrahamse, Recent advances
625 on silver nanoparticle and biopolymer-based biomaterials for wound healing applications, Int.
626 J. Biol. Macromol. 115 (2018) 165–175. doi:10.1016/j.ijbiomac.2018.04.003.
627
628 [14] J. Berger, M. Reist, J.M. Mayer, O. Felt, R. Gurny, Structure and interactions
629 in chitosan hydrogels formed by complexation or aggregation for biomedical applications,
630 Eur. J. Pharm. Biopharm. 57 (2004) 35–52. doi:10.1016/S0939-6411(03)00160-7.
631
632 [15] F.L. Mi, Y.C. Tan, H.C. Liang, R.N. Huang, H.W. Sung, In vitro evaluation of
633 a chitosan membrane cross-linked with genipin, J. Biomater. Sci. Polym. Ed. 12 (2001) 835–
634 850.
635
636 [16] X.F. Liu, Y.L. Guan, D.Z. Yang, Z. Li, K.D. Yao, Antibacterial action of
637 chitosan and carboxymethylated chitosan, J. Appl. Polym. Sci. 79 (2001) 1324–1335.
638 doi:10.1002/1097-4628(20010214)79:7<1324::AID-APP210>3.0.CO;2-L.
639
640 [17] H.K. No, N. Young Park, S. Ho Lee, S.P. Meyers, Antibacterial activity of
641 chitosans and chitosan oligomers with different molecular weights, Int. J. Food Microbiol. 74
642 (2002) 65–72. doi:10.1016/S0168-1605(01)00717-6.
643
644 [18] H. Liu, Y. Du, X. Wang, L. Sun, Chitosan kills bacteria through cell membrane
645 damage, Int. J. Food Microbiol. 95 (2004) 147–155. doi:10.1016/j.ijfoodmicro.2004.01.022.
646
647 [19] Q. Li, X. Wang, X. Lou, H. Yuan, H. Tu, B. Li, Y. Zhang, Genipin-crosslinked
648 electrospun chitosan nanofibers: Determination of crosslinking conditions and evaluation of
649 cytocompatibility, Carbohydr. Polym. 130 (2015) 166–174.
650 doi:10.1016/j.carbpol.2015.05.039.
651
652 [20] H. Tanuma, T. Saito, K. Nishikawa, T. Dong, K. Yazawa, Y. Inoue,
653 Preparation and characterization of PEG-cross-linked chitosan hydrogel films with
654 controllable swelling and enzymatic degradation behavior, Carbohydr. Polym. 80 (2010) 260–
655 265. doi:10.1016/j.carbpol.2009.11.022.

[21] F.-L. Mi, Y.-C. Tan, H.-F. Liang, H.-W. Sung, In vivo biocompatibility and degradability of a novel injectable-chitosan-based implant, Biomaterials. 23 (2002) 181–191.

[22] M. Rinaudo, New way to crosslink chitosan in aqueous solution, Eur. Polym. J. 46 (2010) 1537–1544. doi:10.1016/j.eurpolymj.2010.04.012.

[23] M. Zhang, X.H. Li, Y.D. Gong, N.M. Zhao, X.F. Zhang, Properties and biocompatibility of chitosan films modified by blending with PEG, Biomaterials. 23 (2002) 2641–2648. doi:10.1016/S0142-9612(01)00403-3.

[24] F. Aubert-Viard, A. Martin, F. Chai, C. Neut, N. Tabary, B. Martel, Nicolas Blanchemain, Chitosan finishing nonwoven textiles loaded with silver and iodide for antibacterial wound dressing applications, Biomed. Mater. 10 (2015) 015023.

[25] R.A.A. Muzzarelli, Genipin-crosslinked chitosan hydrogels as biomedical and pharmaceutical aids, Carbohydr. Polym. 77 (2009) 1–9. doi:10.1016/j.carbpol.2009.01.016.

[26] M.F. Butler, Y.-F. Ng, P.D.A. Pudney, Mechanism and kinetics of the crosslinking reaction between biopolymers containing primary amine groups and genipin, J. Polym. Sci. Part Polym. Chem. 41 (2003) 3941–3953. doi:10.1002/pola.10960.

[27] F.-L. Mi, S.-S. Shyu, C.-K. Peng, Characterization of ring-opening polymerization of genipin and pH-dependent cross-linking reactions between chitosan and genipin, J. Polym. Sci. Part Polym. Chem. 43 (2005) 1985–2000. doi:10.1002/pola.20669.

[28] B.. Liu, T.. Huang, A novel wound dressing composed of nonwoven fabric coated with chitosan and herbal extract membrane for wound healing., Polym. Compos. 31 (2010) 1037–1046.

[29] A. Martin, N. Tabary, L. Leclercq, J. Junthip, S. Degoutin, F. Aubert-Viard, F. Cazaux, J. Lyskawa, L. Janus, M. Bria, B. Martel, Multilayered textile coating based on a β-cyclodextrin polyelectrolyte for the controlled release of drugs, Carbohydr. Polym. 93 (2013) 718–730. doi:10.1016/j.carbpol.2012.12.055.

[30] A. Martin, N. Tabary, F. Chai, L. Leclercq, J. Junthip, F. Aubert-Viard, C. Neut, M. Weltrowski, N. Blanchemain, B. Martel, Build-up of an antimicrobial multilayer coating on a textile support based on a methylene blue-poly(cyclodextrin) complex, Biomed. Mater. Bristol Engl. 8 (2013) 065006. doi:10.1088/1748-6041/8/6/065006.

[31] B. Martel, D. Ruffin, M. Weltrowski, Y. Lekchiri, M. Morcellet, Water-soluble polymers and gels from the polycondensation between cyclodextrins and poly(carboxylic acid)s: A study of the preparation parameters, J. Appl. Polym. Sci. 97 (2005) 433–442. doi:10.1002/app.21391.

[32] G. McDonnell, A.D. Russell, Antiseptics and disinfectants: activity, action, and

resistance, Clin. Microbiol. Rev. 12 (1999) 147–179.

[33] J. Langgartner, H.-J. Linde, N. Lehn, M. Reng, J. Schölmerich, T. Glück, Combined skin disinfection with chlorhexidine/propanol and aqueous povidone-iodine reduces bacterial colonisation of central venous catheters, Intensive Care Med. 30 (2004) 1081–1088. doi:10.1007/s00134-004-2282-9.

[34] M. Weltrowski, M. Morcellet, B. Martel, Cyclodextrin polymers and/or cyclodextrin derivatives with complexing properties and ion-exchange properties and method for the production thereof, US6660804B1, 2003. https://patents.google.com/patent/US6660804B1/en (accessed August 27, 2018).

[35] Y. Xue, M. Tang, Y. Hieda, J. Fujihara, K. Takayama, H. Takatsuka, H. Takeshita, High-performance liquid chromatographic determination of chlorhexidine in whole blood by solid-phase extraction and kinetics following an intravenous infusion in rats, J. Anal. Toxicol. 33 (2009) 85–91.

[36] K. Kudo, N. Ikeda, A. Kiyoshima, Y. Hino, N. Nishida, N. Inoue, Toxicological analysis of chlorhexidine in human serum using HPLC on a polymer-coated ODS column, J. Anal. Toxicol. 26 (2002) 119–122.

[37] T. Higuchi, K. Connors, Advances in Analytical Chemistry and Instrumentation., Adv. Anal. Chem. Instrum. (1965) 117–212.

[38] M.E. Brewster, T. Loftsson, Cyclodextrins as pharmaceutical solubilizers, Adv. Drug Deliv. Rev. 59 (2007) 645–666. doi:10.1016/j.addr.2007.05.012.

[39] G. Vermet, S. Degoutin, F. Chai, M. Maton, C. Flores, C. Neut, P.E. Danjou, B. Martel, N. Blanchemain, Cyclodextrin modified PLLA parietal reinforcement implant with prolonged antibacterial activity, Acta Biomater. 53 (2017) 222–232. doi:10.1016/j.actbio.2017.02.017.

[40] L. Gao, H. Gan, Z. Meng, R. Gu, Z. Wu, X. Zhu, W. Sun, J. Li, Y. Zheng, T. Sun, G. Dou, Evaluation of genipin-crosslinked chitosan hydrogels as a potential carrier for silver sulfadiazine nanocrystals, Colloids Surf. B Biointerfaces. 148 (2016) 343–353. doi:10.1016/j.colsurfb.2016.06.016.

[41] M.P. Klein, C.R. Hackenhaar, A.S.G. Lorenzoni, R.C. Rodrigues, T.M.H. Costa, J.L. Ninow, P.F. Hertz, Chitosan crosslinked with genipin as support matrix for application in food process: Support characterization and β-d-galactosidase immobilization, Carbohydr. Polym. 137 (2016) 184–190. doi:10.1016/j.carbpol.2015.10.069.

[42] A.S. Vikulina, Y.G. Anissimov, P. Singh, V.Z. Prokopović, K. Uhlig, M.S. Jaeger, R. von Klitzing, C. Duschl, D. Volodkin, Temperature effect on the build-up of

exponentially growing polyelectrolyte multilayers. An exponential-to-linear transition point, Phys. Chem. Chem. Phys. 18 (2016) 7866–7874. doi:10.1039/C6CP00345A.

[43] L. Richert, P. Lavalle, E. Payan, X.Z. Shu, G.D. Prestwich, J.-F. Stoltz, P. Schaaf, J.-C. Voegel, C. Picart, Layer by Layer Buildup of Polysaccharide Films: Physical Chemistry and Cellular Adhesion Aspects, Langmuir. 20 (2004) 448–458. doi:10.1021/la035415n.

[44] B. Seantier, A. Deratani, Polyelectrolytes at Interfaces: Applications and Transport Properties of Polyelectrolyte Multilayers in Membranes, in: Ion. Interact. Nat. Synth. Macromol., Wiley-Blackwell, 2012: pp. 683–726. doi:10.1002/9781118165850.ch18.

[45] G. Ladam, P. Schaad, J.C. Voegel, P. Schaaf, G. Decher, F. Cuisinier, In Situ Determination of the Structural Properties of Initially Deposited Polyelectrolyte Multilayers, Langmuir. 16 (2000) 1249–1255. doi:10.1021/la990650k.

[46] F. Caruso, D.N. Furlong, K. Ariga, I. Ichinose, T. Kunitake, Characterization of Polyelectrolyte−Protein Multilayer Films by Atomic Force Microscopy, Scanning Electron Microscopy, and Fourier Transform Infrared Reflection−Absorption Spectroscopy, Langmuir. 14 (1998) 4559–4565. doi:10.1021/la971288h.

[47] S. Ouerghemmi, S. Degoutin, N. Tabary, F. Cazaux, M. Maton, V. Gaucher, L. Janus, C. Neut, F. Chai, N. Blanchemain, B. Martel, Triclosan loaded electrospun nanofibers based on a cyclodextrin polymer and chitosan polyelectrolyte complex, Int. J. Pharm. 513 (2016) 483–495. doi:10.1016/j.ijpharm.2016.09.060.

[48] Y.-T. Lau, L.-F. Kwok, K.-W. Tam, Y.-S. Chan, D.K.-Y. Shum, G.K.-H. Shea, Genipin-treated chitosan nanofibers as a novel scaffold for nerve guidance channel design, Colloids Surf. B Biointerfaces. 162 (2018) 126–134. doi:10.1016/j.colsurfb.2017.11.061.

[49] N.E. Muzzio, M.A. Pasquale, E. Diamanti, D. Gregurec, M.M. Moro, O. Azzaroni, S.E. Moya, Enhanced antiadhesive properties of chitosan/hyaluronic acid polyelectrolyte multilayers driven by thermal annealing: Low adherence for mammalian cells and selective decrease in adhesion for Gram-positive bacteria, Mater. Sci. Eng. C Mater. Biol. Appl. 80 (2017) 677–687. doi:10.1016/j.msec.2017.07.016.

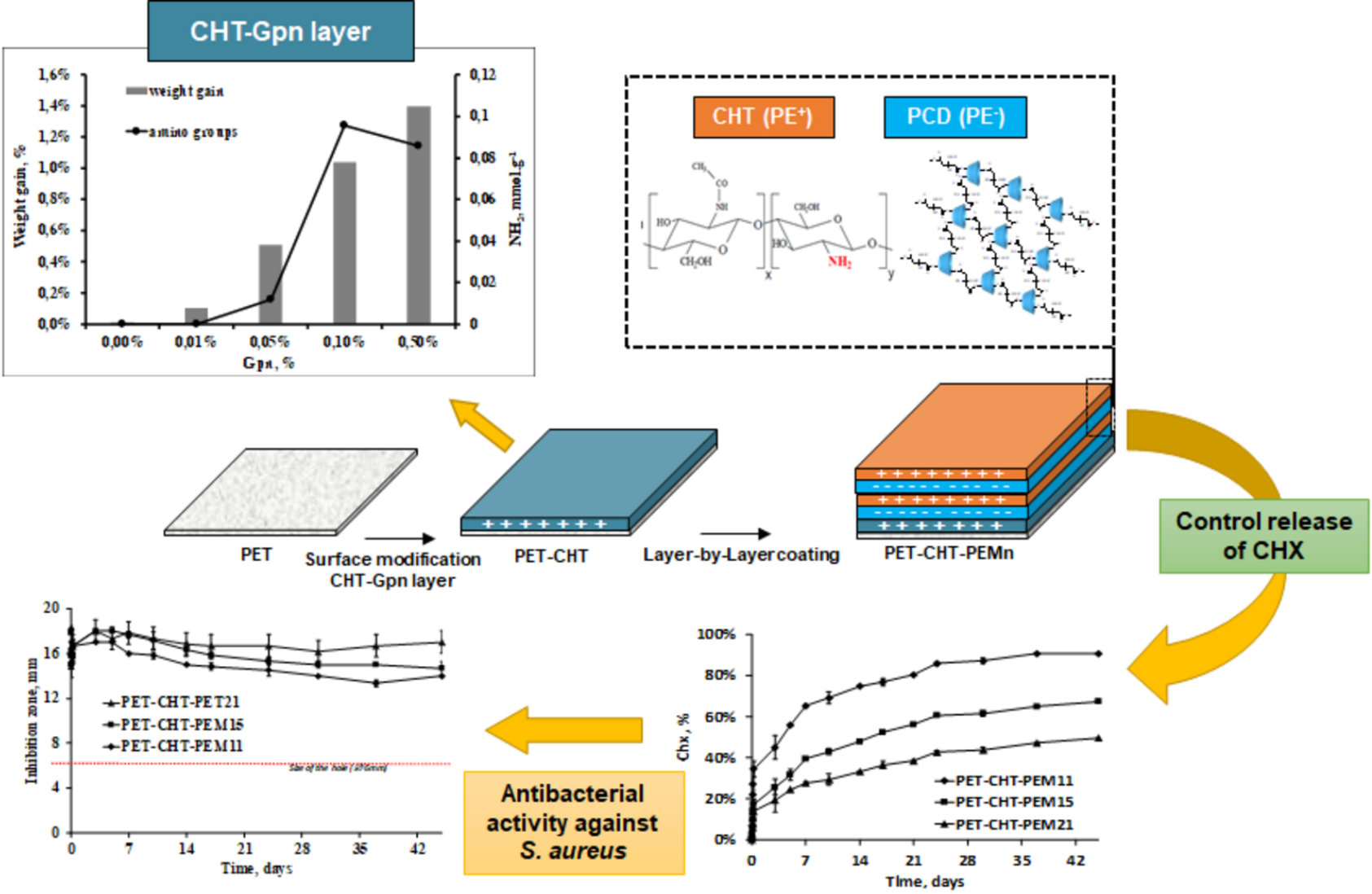
[50] P. Saokham, C. Muankaew, P. Jansook, T. Loftsson, Solubility of Cyclodextrins and Drug/Cyclodextrin Complexes, Mol. Basel Switz. 23 (2018). doi:10.3390/molecules23051161.

[51] N. Tabary, F. Chai, N. Blanchemain, C. Neut, L. Pauchet, S. Bertini, E. Delcourt-Debruyne, H.F. Hildebrand, B. Martel, A chlorhexidine-loaded biodegradable cellulosic device for periodontal pockets treatment, Acta Biomater. 10 (2014) 318–329. doi:10.1016/j.actbio.2013.09.032.

[52] J. Junthip, N. Tabary, F. Chai, L. Leclercq, M. Maton, F. Cazaux, C. Neut, L. Paccou, Y. Guinet, J.-N. Staelens, M. Bria, D. Landy, A. Hédoux, N. Blanchemain, B. Martel, Layer-by-layer coating of textile with two oppositely charged cyclodextrin polyelectrolytes for extended drug delivery, J. Biomed. Mater. Res. A. 104 (2016) 1408–1424. doi:10.1002/jbm.a.35674.

[53] E. Diamanti, N. Muzzio, D. Gregurec, J. Irigoyen, M. Pasquale, O. Azzaroni, M. Brinkmann, S.E. Moya, Impact of thermal annealing on wettability and antifouling characteristics of alginate poly-l-lysine polyelectrolyte multilayer films, Colloids Surf. B Biointerfaces. 145 (2016) 328–337. doi:10.1016/j.colsurfb.2016.05.013.

[54] N. Lavoine, N. Tabary, I. Desloges, B. Martel, J. Bras, Controlled release of chlorhexidine digluconate using β-cyclodextrin and microfibrillated cellulose, Colloids Surf. B Biointerfaces. 121 (2014) 196–205. doi:10.1016/j.colsurfb.2014.06.021.


CHT-Gpn layer
weight gain
amino groups
Weight gain, %
NH_2, mmol·g^{-1}
Gpn, %
CHT (PE$^+$)
PCD (PE$^-$)
PET
Surface modification
CHT-Gpn layer
PET-CHT
Layer-by-Layer coating
PET-CHT-PEMn
Control release of CHX
Antibacterial activity against *S. aureus*
Inhibition zone, mm
Time, days
PET-CHT-PET21
PET-CHT-PEM15
PET-CHT-PEM11
Chx, %
Time, days
PET-CHT-PEM11
PET-CHT-PEM15
PET-CHT-PEM21